Bioresource Technology 133 (2013) 482–494

Contents lists available at SciVerse ScienceDirect

Bioresource Technology

journal homepage: www.elsevier.com/locate/biortech

Mathematical modeling of poly[(*R*)-3-hydroxyalkanoate] synthesis by *Cupriavidus necator* DSM 545 on substrates stemming from biodiesel production

Ivna Vrana Špoljarić [a], Markan Lopar [a], Martin Koller [b], Alexander Muhr [b], Anna Salerno [b], Angelika Reiterer [b], Karin Malli [b], Hannes Angerer [b], Katharina Strohmeier [c], Sigurd Schober [c], Martin Mittelbach [c], Predrag Horvat [a,*]

[a] *Department of Biochemical Engineering, Faculty of Food Technology and Biotechnology, University of Zagreb, Pierottijeva 6/IV, HR-10000 Zagreb, Croatia*
[b] *Institute of Biotechnology and Biochemical Engineering, Graz University of Technology, Petersgasse 12, A-8010 Graz, Austria*
[c] *Institute of Chemistry, University of Graz, Heinrichstraße 28, A-8010 Graz, Austria*

HIGHLIGHTS

- Valuable mathematical models for PHA production by *Cupriavidus necator* on combined substrates.
- PHA production on waste substrates from biodiesel (FAME and glycerol).
- New low structured model for fed-batch fermentation on glucose with glycerol.
- New low structured model for fed-batch fermentation on FAME with valeric acid.
- *In silico* optimized feeding of C-sources and PHB/PHBV content by mathematical models.

ARTICLE INFO

Article history:
Received 21 November 2012
Received in revised form 21 January 2013
Accepted 22 January 2013
Available online 31 January 2013

Keywords:
Cupriavidus necator
Biodiesel
Polyhydroxybutyrate (PHB)
Poly[hydroxybutyrate-co-hydroxyvalerate] (PHBV)
Mathematical modeling

ABSTRACT

Two low structured mathematical models for fed-batch production of polyhydroxybutyrate and poly[hydroxybutyrate-co-hydroxyvalerate] by *Cupriavidus necator* DSM 545 on renewable substrates (glycerol and fatty acid methyl esters-FAME) combined with glucose and valeric acid, were established. The models were used for development/optimization of feeding strategies of carbon and nitrogen sources concerning PHA content and polymer/copolymer composition. Glycerol/glucose fermentation featured a max. specific growth rate of 0.171 h^{-1}, a max. specific production rate of 0.038 h^{-1} and a PHB content of 64.5%, whereas the FAME/valeric acid fermentation resulted in a max. specific growth rate of 0.046 h^{-1}, a max. specific production rate of 0.07 h^{-1} and 63.6% PHBV content with 4.3% of 3-hydroxyvalerate (3HV) in PHBV. A strong inhibition of glycerol consumption by glucose was confirmed (inhibition constant $k_{i,G} = 4.28 \times 10^{-4}$ g L^{-1}). Applied concentration of FAME (10–12 g L^{-1}) positively influenced on PHBV synthesis. HV/PHBV ratio depends on applied VA concentration.

1. Introduction

Polyhydroxyalkanoates (PHAs) are biodegradable polymers with similar material properties like petrochemical plastics (Braunegg et al., 2007; Lee, 1996; Steinbüchel and Doi, 2001). These biopolymers can be produced by different bacterial and archaebacterial species and genetically modified plants (Sudesh et al., 2000). In bacteria, PHAs are produced under nutritional stress conditions like nitrogen or phosphate limitation together with excess carbon source in the cultivation broth. In dependence of different carbon sources microorganisms can accumulate various types of PHAs. They can be produced in the form of homopolyesters, copolyesters, terpolyesters or as polyester blends. PHA is stored in the cell cytoplasm of bacteria in the shape of granules usually with diameter between 0.2 and 0.5 μm (Sudesh et al., 2000). Bacterial polymers have auspicious future perspective for replacing petrochemical plastic; as a pre-condition, the production price has to decrease. Therefore, contemporary, different organic wastes are examined as raw materials for PHA production. Beside the fact that this type of bioplastics is eco-friendly (those molecules are completely biodegradable), its production from waste material can be the part of solution of waste disposal problems (Braunegg et al., 2007; Koller et al. 2005).

* Corresponding author. Tel.: +385 1 46 05 166; fax: +385 1 48 36 424.
E-mail address: phorvat@pbf.hr (P. Horvat).

0960-8524/$ - see front matter © 2013 Elsevier Ltd. All rights reserved.
http://dx.doi.org/10.1016/j.biortech.2013.01.126

PHAs can be composed of up to 150 different compounds (Steinbüchel and Lütke-Eversloh, 2003); the best-known members are poly ([*R*]-3-hydroxybutyrate) (PHB) and the copolyester poly ([R]-3-hydroxybutyrate -co-3-hydroxyvalerate) (PHBV). In general, PHAs can be classified in two main groups. The first group encompasses short chain length PHAs (*scl*-PHAs) with chain lengths of the monomers from C_3 to C_5 (i.e. PHB and PHBV); the production of these polyesters is best investigated by the wild type strain *Cupriavidus necator* (Khanna and Srivastava, 2005; Steinbüchel and Valentin, 1995; Sudesh et al., 2000). The second group consists of medium chain length PHA (*mcl*-PHA) with chain lengths from C_6 to C_{14}; these types of copolymers are mainly produced by *Pseudomonas* species (Khanna and Srivastava, 2005; Steinbüchel and Valentin, 1995). Today it's well known that the monomeric composition of copolymers (e.g. 3HB co-polymerization) with different monomer units like 3-hydroxyvalerate (3HV) or 4-hydroxybutyrate (4HB) units affects the final properties (quality) of the polymer product (Madison and Huisman, 1999). For example, the thermo-mechanical properties of the copolymer PHBV depend on their 3HV content (Lefebvre et al. 1997). Enhanced PHA properties, e.g. lower melting points, decreased crystallinity, can most conveniently be obtained by triggering the supply of carbon source/s by adding of different precursors to the fermentation broth (Aldor and Keaslingy, 2003). The bacterium *C. necator* produces different types of PHA biopolymers dependent on the carbon source supply. This producer synthesizes *scl*-PHA from sugars and some organic acids through the Entner–Doudoroff pathway and/or gluconeogenesis (Kaddor and Steinbüchel, 2011; Tanadchangsaeng and Yu, 2012), while *mcl*-PHA is accessible by the catalytic action of various pseudomonad strains through fatty acid β-oxidation when *mcl*-fatty acids are provided as carbon sources (Lageveen et al. 1988). In addition, PHB is usually produced from carbon sources like glucose and/or even-numbered fatty acids, whereas PHBV is accessible from carbon sources like odd-numbered fatty acids, propionic or valeric acid, mixtures of acetic and propionic acid, or a mixture of fructose with valeric acid (Kelley et al., 2001). Furthermore, PHBV is produced by providing carbon sources like sodium 4-hydroxybutyrate, 1,4-butanediol, or γ-butyrolactone, whereas polymers containing the rare building block 4-hydroxyvalerate (4HV), mainly the terpolyester P(3HB-co-3HV-co-4HV) are accessible by providing levulinic acid as sole or additional carbon source to *C. necator* (Du et al., 2001; Gorenflo et al., 2001; Yu and Si, 2004).

For the work at hand, PHA production by *C. necator* DSM 545 on carbon sources predominantly originated from biodiesel production was investigated. Here, two main waste streams from biodiesel production were utilized: glycerol (GLY) and saturated fatty acid methyl esters (FAME). Fed-batch cultivations for PHA production from glucose (G) combined with glycerol (GLY/G), as well as from saturated biodiesel (FAME) combined with valeric acid (VA) (FAME/VA) were performed.

Biodiesel is a mixture of fatty acids methyl esters (FAME) produced via transesterification of vegetable oils or animal fats (Cavalheiro et al., 2009). *C. necator*, *Azahydromonas lata* and *Burkholderia sacchari* as wild strains and recombinant strains of *C. necator* and *Escherichia coli* (Lemos et al., 2006; Khanna and Srivastava, 2005; Vandamme and Coenye, 2004) are today identified as the most promising PHA producers regarding volumetric productivities, substrate spectrum and polyester properties. Among them, *C. necator* is the best studied producer of PHA with a completely sequenced genome (Reinecke and Steinbuchel, 2009). This strain can produce PHA from various and structurally completely different carbon substrates: it can be cultivated lithoautotrophically on mixtures of CO_2 and H_2, but also heterotrophically on organic carbon substrates like fructose, glucose, glycerol, plant oil, palm oil, biodiesel, and volatile fatty acids like lactate, butyrate, acetate, propionate or valerate. Beside the carbon source that is decisive both for microbial growth and PHA biosynthesis, it is very important to ensure sufficient supply with nitrogen and phosphorus source during the growth phase. An insufficient supply with the last two mentioned substrates can be regarded as the main regulating factor for redirection of carbon flux from biomass to PHA synthesis. Hence, it is crucial to assess the optimum of C/N ratio (Chakraborty et al., 2009; Zinn et al., 2004) for best production of PHA at non-growth associated conditions.

It is well-known that the formation of PHB can be comprehended as a microbial strategy to regenerate reducing power by transferring hydrogen from NADH to acetoacetyl-CoA, generating NAD^+ and 3-hydroxybutyryl-CoA; this is catalyzed by the action of acetoacetyl-CoA reductase. In contrast to recently reported findings with *Rhodopseudomonas palustris* WP3-5 (Wu et al., 2012), the production strain *C. necator* used in the presented study, if cultivated on organic acids, does not possess the concurring pathway of generating reducing power by release of molecular hydrogen; hence, PHB production is the strains predominant pathway to recover NAD^+ under nutrient limiting condition, resulting in higher PHA productivity on FAMEs in comparison to e.g. *R. palustris* WP3-5. Furthermore it was reported that ions of metals influenced the PHB synthesis and uptake, so phosphate accumulating microorganisms (PAOs) could normally synthesize polyhydroxybutyrate (PHB) in the anaerobic phase even though lead concentration was 40 mg L^{-1}. However, they could not aerobically utilize PHB normally in the presence of lead (You et al., 2011), but glycogen accumulating organisms (GAOs) could not normally metabolize polyhydroxyvalerate (PHV) in both the anaerobic and aerobic phases.

The achieved content of PHA in cell dry mass (CDM) is a crucial parameter for the industrial feasibility of a PHA production process, especially regarding the downstream processing after the biosynthesis, and is also depending on the applied carbon source and feeding strategy. By using different C/N ratios and fermentation techniques, the final PHA content and the volumetric productivity for PHA can be improved. In addition, the applied carbon source also impacts the properties of the obtained polyester; in the case of polyols like glycerol, lower molecular masses are obtained than by using sugars due to termination of the propagation of growing polymer chains (reviewed by Koller et al., 2005).

The applied substrates are decisive for specific growth rate, productivity and PHA yield by *C. necator*. This can be understood by the fact that different substrates are transported inside the cells by different transport systems and metabolized by related metabolic pathways. These indicators for the process performance are usually higher when glucose acts as C-source than in the case of glycerol or fatty acids. Glucose is actively channeled into the cells by the phosphoenolpyruvate-carbohydrate phosphotransferase system (PEP-PTS); it is phosphorylated during transport and catabolized through the Entner–Doudoroff pathway (Raberg et al., 2011), while glycerol and fatty acids are transported across the cytoplasmic membrane by facilitated diffusion (Sweet et al., 1990). Intracellular glycerol has to be phosphorylated by the catalytic aid of glycerol kinase and oxidized by glycerol-3-phosphate dehydrogenase. Also in the case of glycerol utilization, gluconeogenesis serves as the main metabolic pathway for biosynthesis of desired cellular components. In addition, fatty acids have to be activated by coenzyme A (CoA) before getting metabolized by the β-oxidation pathway (Brigham et al., 2010). By each circle of β-oxidation, the fatty acid gets shortened by 2 carbon units, so different chain lengths of fatty acids are present in the cell and can be incorporated in the growing PHA biopolymer chain.

Furthermore, high concentrations of glycerol and FAMEs are known to display toxic effects on the producing microorganism. For biosynthesis of cellular components, the so called glyoxylate

bypass plays a major role; as its main product, phosphoenolpyruvate (PEP) is generated (Brigham et al., 2010). Phosphorylation of glycerol by glycerol kinase and activation of fatty acids by coupling to CoA before getting metabolized take longer time than the direct phosphorylation of glucose during the import into the cells. Hence, PHA production occurs at slower rates on glycerol and FAMEs than on glucose. In addition, metabolic pathways (gluconeogenesis and β-oxidation with glyoxylate bypass) for the synthesis of the biomass components contribute to longer lag phase and consequently to lower productivity.

The main goal of this work was to determine kinetic properties of *C. necator* DSM 545 growing on renewable substrates originated predominantly from biodiesel production (GLY/G fermentation and FAME/VA fermentation), to establish low structured kinetic models for PHA synthesis on those substrates and to optimize feeding strategy and PHA content by the help of established models. The final target of this work was to reduce the amount of necessary experimental work and to find the best feeding strategy for both fermentations. Generally, mathematical models are powerful tools for such actions; here, formal-kinetic, low structured, high structured metabolic or cybernetic models can be established and applied. Intended for industrial implementation of data elaborated on laboratory scale, simplified mathematical metabolic models (i.e. low structured, formal kinetic models) were chosen for the work at hand as fast and practical tool for daily laboratory research praxis. In literature different structured and unstructured mathematical models can be found for PHA productions performed by batch, fed-batch and continuous fermentations using different substrates and *C. necator* as microbial production strain. According to our knowledge, this study is the first reported work dealing with formal kinetics and low structured models of PHA production by *C. necator* DSM 545 on glucose combined with glycerol as well as on fatty acids methyl esters (from biodiesel) combined with valeric acid.

2. Methods

2.1. Microorganism

Working microorganism *C. necator* (DSM 545) was obtained from DSMZ (Deutsche Sammlung von Mikroorganismen und Zellkulturen GmbH), Braunschweig, Germany as vacuum-dried culture. The strain was revitalized and cultivated using the nutritional medium according to (Küng, 1982) containing (per liter): Na_2HPO_4, 3.59 g; KH_2PO_4, 1.5 g; $MgSO_4{\cdot}7H_2O$, 0.2 g; $(NH_4)_2SO_4$, 2 g; $CaCl_2{\cdot}2H_2O$, 0.02 g; NH4Fe(III)citrate, 0.05 g; trace element solution SL6, 1 mL; glycerol, 10 g. The trace element solution SL6 was composed as follows (per liter): $ZnSO_4{\cdot}7H_2O$, 100 mg; H_3BO_3, 300 mg; $CoCl_2{\cdot}6H_2O$, 200 mg; $CuSO_4$, 6 mg; $NiCl_2{\cdot}6H_2O$, 20 mg; $Na_2MoO_4{\cdot}2H_2O$, 30 mg; $MnCl_2{\cdot}2H_2O$, 25 mg.

2.2. Analytical procedures

2.2.1. Determination of cell dry mass (CDM)

A gravimetric method was used to determine the biomass concentration expressed as CDM in fermentation samples. 5 mL of culture broth were centrifuged in pre-weighed glass screw-cap tubes for 10 min at 10 °C and 4000 rcf in Heraeus Megafuge 1.0 R refrigerated centrifuge. The supernatant was decanted and used for substrate analysis. The cell pellets were washed with distilled water, re-centrifuged, frozen and lyophilized to a constant mass. CDM was determined as the mass difference between the tubes containing cell pellets and empty tubes. The determination was done in duplicate. The lyophilized pellets were subsequently used for determination of intracellular PHA as described below. Residual biomass (non-PHB part of biomass) was calculated by subtracting of PHA mass from CDM mass.

2.2.2. PHA analysis

PHA in lyophilized biomass samples was transesterificated by acidic methanolysis (Braunegg et al., 1978). The gas chromatographic analysis was performed with a 6850 Network GC System (Agilent Technologies), equipped with a 25 m × 0.32 mm × 0.52 μm HP5 capillary column and a flame ionization detector (FID). Helium (Linde; purity = 4.6) was used as carrier gas with a split-ratio of 1:5, hydrogen (Linde; purity = 5.0) and synthetic air (Linde; purity = "free of hydrocarbons") as detector gases and nitrogen (Linde; purity = 5.0) as auxiliary gas. The following protocol for the temperature program was used: Initial temperature: 50 °C; rate 1:15 °C min^{-1}; final temperature 1:60 °C; rate 2:2 °C min^{-1}; final temperature 2:80 °C; final temperature 3:300 °C; final time 3:5 min. The determination of all samples was done in duplicate. The methyl esters of PHA constituents were detected by a flame ionization detector (FID); carrier gas: helium (split-ratio of 1:10), injection volume of 1 μL. The copolyester Poly(3HB-*co*-15.6%-3HV) (BIOPOL™, ICI, UK) was used as reference material, hexanoic acid acted as internal standard. The PHA content (wt.%) was defined as the percentage of PHA concentration to dry cell mass (CDM).

2.2.3. Ammonia determination

A commercially available test (Merck, Spectroquant, 1.00683.0001) was used, following the principle of ammonia reacting with hypochlorite ions to monochloramine, which further reacts with substituted phenol to form a blue indophenol derivative. This complex can be determined photometrically at 690 nm. The measuring range of the test for ammonium is 6–193 mg L^{-1}. Ammonium sulphate was used as reference. After the centrifugation of the tubes from sampling, the supernatants of the parallel tubes were combined and an aliquot was filtrated for the ammonium test. Firstly, 5 mL of NH4-1 reagent were mixed with 0.1 mL of sample. Secondly, 1 level blue micro-spoon NH4-2 was added and the solution was mixed until the reagent was dissolved. The initial solution was left to stand for 15 min (reaction time) and measured in a 10-mm cell at 690 nm. Deionized water was used as zero reference.

2.2.4. Glycerol, glucose and valerate determination

Glycerol, glucose and valerate concentration in supernatant (remaining after the centrifugation step described in Section 2.2.1) was monitored using a high-performance liquid chromatography (HPLC; *Shimadzu*) equipment consisting of a thermostated Aminex HPX 87H column (thermostated at 75 °C, Biorad, Hercules, USA), a LC-20AD pump, a SIC-20 AC auto-sampler, a RID-10A refractive index detector and a CTO-20 AC column oven. For registration and evaluation of the data, LC solution software was used. Sterile-filtrated supernatant was transferred into vials and water was used as eluent at a flow rate of 0.6 mL min^{-1}. External standards were prepared using different concentrations of p.a. glycerol (Fluka), sodium valerate (Merck) or p.a. glucose (Fluka), respectively.

2.2.5. Biofuel monitoring

The fatty acid composition of the biodiesel used as feedstock for the fermentation FAME/VA and of the residual biodiesel in the supernatants of the samples deriving from this fermentation process were determined by gas liquid chromatography on a HP 7890 GC apparatus equipped with a flame ionization detector (GC-FID), according to a standard procedure (AOCS Ce 1-62). Chromatographic separation of the individual fatty acid esters was performed on a DB wax column (30 m × 0.25 mm × 0.15 μm). Helium was used as carrier gas (constant flow of 0.7 mL min^{-1}) and 1 × μL

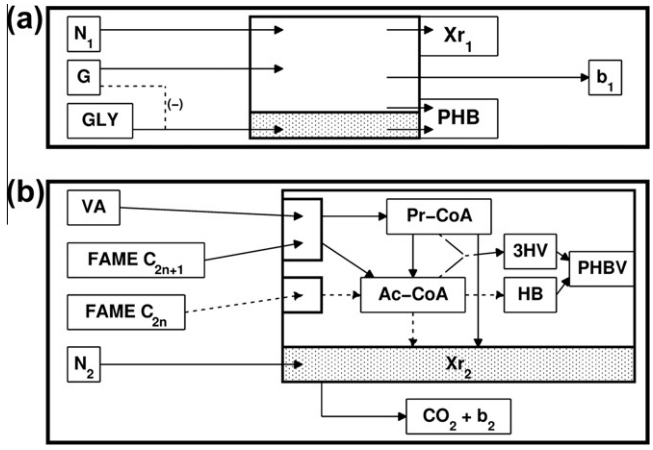

Fig. 1. Simplified metabolic reaction network for *Cupriavidus necator* DSM 545 and material fluxes applied in: formal kinetic model (FKM1) for PHB synthesis from glucose (G) with glycerol (GLY); (b) FKM2 of PHBV synthesis from FAME with valeric acid (VA).

of the sample was injected. The identification of the peaks was done by comparison of the retention times to a reference material (GLC-462, Nu Check Prep Inc). The fatty acid concentration was calculated by using methyl nonadecanoate (Fluka) as an internal standard according to (AOCS Ce 1-62). The supernatants samples have to be converted into methyl esters prior to analysis. This is carried out according to (AOCS Ce 2-66).

2.3. Cultivation procedure

2.3.1. Fed-batch fermentation on glucose with glycerol (GLY/G) by C. necator DSM 545

The strain was transferred to new solid media plates (medium according to Küng with 10 g L^{-1} of glucose as carbon source and 2 g L^{-1} ammonium sulfate as nitrogen source) and incubated for 2 days at 37 °C. From these plates, selected colonies were used to inoculate 3 × 100 mL media (pre-cultures) of the medium according to Küng (Chapter 2.1). The pre-cultures were left to incubate (37 °C) for approximately 24 h and then 5 mL of the pre-cultures were used for inoculate each 7 × 250 mL with the same medium composition as the pre-cultures (inoculum for the bioreactor experiment). The inoculum flasks were incubated at 37 °C for another 24 h. A Labors3 bioreactor (Infors, CH; equipped with two axial impeller stirrers agitation from the top of the reactor) was used for the cultivation. The applied cultivation conditions were as follows: pH-value = 7.0; T = 37 °C; initial glycerol concentration approximately 50 g L^{-1}; initial glucose concentration appr. 40 g L^{-1} (stepwise addition), growth limiting factor: nitrogen source (NH_4^+). The additions of nitrogen source were carried out using NH_4OH as base. After 18.5 h of fermentation, NH_4OH was exchanged by NaOH in order to come to nitrogen limited conditions that occurred after 25.5 h of cultivation. Glycerol was only provided at the beginning of the cultivation, glucose additions (50% aqueous solution) were done according to analytical results as illustrated in Fig. 2. After stop of the fermentation (t = 58 h), the fermentation broth was in situ pasteurized, harvested, and centrifuged. The obtained bacterial biomass was frozen, lyophilized and subjected to extraction of the polymer as described before (Braunegg et al., 1978).

2.3.2. Fed-batch fermentation on FAME with VA (FAME/VA) by C. necator DSM 545

The strain was cultivated on solid media plates (medium according to Küng with 5 g L^{-1} of biodiesel as carbon source and 3 g L^{-1} ammonium sulfate as nitrogen source) at 37 °C. From these plates, selected colonies were used to inoculate 3 × 100 mL media (pre-cultures) of the medium according to Küng containing (per liter): Na_2HPO_4, 4.8 g; KH_2PO_4, 2 g; $MgSO_4{\cdot}7H_2O$, 0.5 g; $(NH_4)_2SO_4$, 3 g; $CaCl_2{\cdot}2H_2O$, 0.02 g; NH4Fe(III)citrate, 0.05 g; trace element

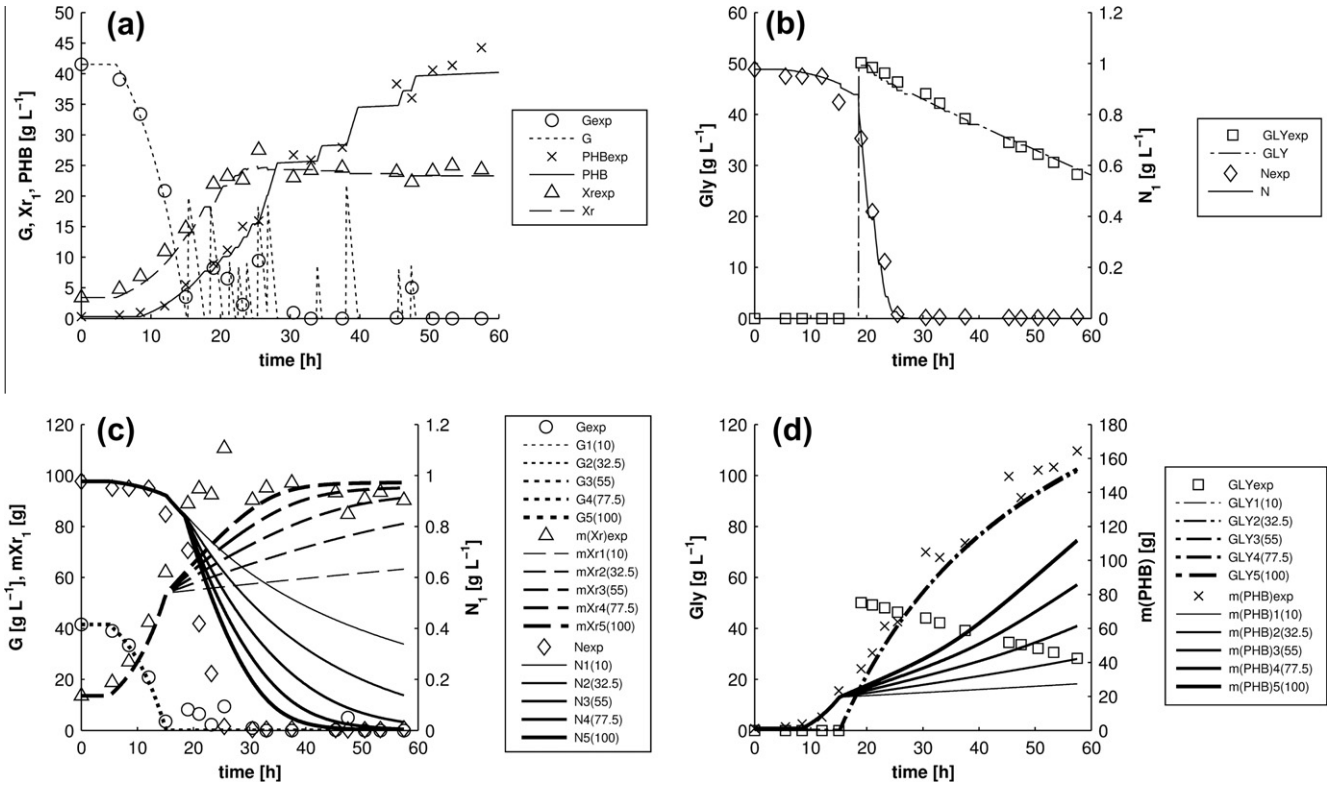

Fig. 2. Experimental and simulated data (FKM1) of PHB production on GLY/G by *Cupriavidus necator* DSM 545: (a and b) model validation and (c and d) *in silico* fermentations.

solution SL6, 5 mL. The SL6 solution was composed as described in Chapter 2.1. The pre-cultures were left to incubate (37 °C) for approximately 24 h and then 5 mL of the pre-cultures were used for inoculate each 12 × 250 mL with the same medium composition as the pre-cultures (inoculum for the bioreactor experiment). The inoculum flasks were incubated at 37 °C for another 24 h. A Labors3 bioreactor (Infors, CH; equipped with two axial impeller stirrers agitation from the top of the reactor) was used for the cultivation. The applied cultivation conditions were as follows: pH-value = 7.0; T = 37 °C; initial biodiesel concentration approximately 10 g L^{-1}; growth limiting factor: nitrogen source (NH_4^+). The additions of nitrogen source were carried out using NH_4OH as base. Biodiesel was added on the beginning of cultivation (12.5 g L^{-1}), and if needed, in the accordance to the substrate consumption that goes in parallel with the monitored oxygen consumption (due to demand of the microorganisms). After 64 h of fermentation, NH_4OH was exchanged by NaOH in order to achieve nitrogen limited conditions, which occurred after 72 h of cultivation. At this point, for every further addition of 2 mL biodiesel, 1 mL valeric acid solution (20%) was added (ratio biodiesel to valeric acid 1:10) as precursor for the production of 3HV. After ending the fermentation (t = 91 h), the fermentation broth was in situ pasteurized at 70 °C for 1 h, harvested, and centrifuged. The obtained bacterial biomass was frozen, lyophilized and subjected to extraction of the polymer as described before.

2.4. Kinetic analysis and modeling principle

Kinetic parameters as specific growth rates and specific production rates as well as yield coefficients for residual biomass and for PHA were estimated from related fermentation data by standard procedures of bioprocess kinetics (Moser, 1988).

2.4.1. Modeling principles for PHB production by C. necator DSM 545 on GLY/G

Modeling principles for PHB production under N-limited conditions when as a carbon source were used glucose with glycerol (Fig. 1a):

(a) Residual biomass (Xr_1) is synthesized only from glucose when nitrogen source is available (the growth on glycerol in presence of glucose is approached as practically negligible).
(b) Duration of the lag-phase of 5 h was assumed.
(c) PHB is synthesized from two carbon source, glucose and glycerol. In the exponential phase of growth it was assumed that the PHB synthesis from glucose is growth associated type with time delay of 3.5 h after beginning of exponential growth phase. In the fed-batch part of fermentation and in the stationary phase of growth, the PHB synthesis from glucose is redirected to the growth non-associated type and the nitrogen source depletion was assumed to be an activator of growth non-associated type of synthesis. The synthesis of PHB from GLY was assumed to be a growth non-associated type, having maximal rate (high GLY concentration!), but inhibited and by factor "r" powered inhibition if glucose is present in the broth.
(d) Maintenance energy (b_1) is generated by metabolism of glucose.
(e) Nitrogen source was added for the pH correction and the quantity is assumed to be proportional to the growth rate in the exponential phase.

2.4.2. Modeling principles for PHBV production by C. necator on FAME/VA

Modeling principles for PHBV production under N-limited conditions when FAME and VA were used as carbon sources (Fig. 1b):

(a) Total biomass (CDM_2) is divided in two "compartments": residual biomass (Xr_2) and polyhydroxyalkanoate (PHBV). PHBV contains 3-hydroxybutyrate (HB) and 3-hydroxyvalerate (3HV) monomers;
(b) Residual biomass (Xr_2) (non-PHA part of biomass) is synthesized only from biodiesel (FAME) and ammonia (as C and N source) because valeric acid was added in non-growth phase. Growth of Xr_2 was assumed to be limited by nitrogen source. In the same time the FAME and the VA were anticipated as sources for the maintenance energy (b_2). Furthermore, it was assumed (based on experimental data!) that duration of lag phase is 37 h.
(c) PHBV is divided in two "sub-compartments": HB and 3HV.
(d) HB is synthesized from biodiesel particular during the growth phase (growth associated HB synthesis) and dominantly during the non-growth phase (non-growth associated HB synthesis)
(e) 3HV is synthesized only from VA during the non-growth phase (non-growth associated 3HV synthesis). Conversion of FAME in 3HV was not detected in growth phase;
(f) A part of carbon sources (FAME and VA) are spent for synthesis of CO_2 and other minor metabolites.

2.5. Mathematical model and value of model parameters

2.5.1. Mathematical model (FKM1) for PHB production by C. necator on GLY/G

Based on modeling principles, the appropriate formal kinetic model (FKM1) for PHB production on GLY/G was established. Eq. (1) assumed that total biomass (CDM_1) is the sum of residual biomass (Xr_1) and PHB concentration. Residual biomass growth (Xr_1) is defined by Eq. (2) and includes lag phase (t_L) that last 5 h. PHB mass balance equation (Eq. (3)) includes growth associated PHB synthesis (from G in presence of N source), growth non-associated synthesis from G and growth non-associated synthesis from GLY. Glucose mass balance equation (Eq. (4)) includes consumption terms for: biomass growth, PHB synthesis during the growth phase, PHB synthesis during the N limited phase, and glucose consumption for maintenance energy production. Glycerol mass balance equation (Eq. (5)) contains terms related to glycerol consumption for PHB synthesis and to residual biomass growth. Nitrogen mass balance equation (Eq. (6)) includes nitrogen consumption term related to biomass synthesis and term for pH regulation by NH_4OH. All balance equations (i.e. for residual biomass (Xr_1, PHB, glucose, glycerol and nitrogen sources) have incorporated terms related to substrates feeding and analytical sampling. Specific growth rate of biomass (μ_G) on glucose (Eq. (7)) is defined according to the "two substrate" kinetic equation (known as "double Monod" relation). Specific non-growth associated PHB production rate (q_G) on glucose (Eq. (9)) is set to be nitrogen inhibited (nitrogen concentration has inhibitory effect on PHA synthesis from glucose). Specific non-growth associated PHA production rate (q_{GLY}) on glycerol (Eq. (10)) is set to be regulated by glucose concentration (glucose has inhibitory effect on glycerol uptake for PHB synthesis). Specific consumption rate for maintenance energy (b_1) is substrate dependent according to Monod equation (Eq. (11)). Concentrations of glucose (G), glycerol (GLY), residual biomass (Xr_1), PHB, nitrogen (N_1) and cell dry mass (CDM_1) were calculated from mass to volume ratio according to following equation: $c_i = m_{i(t)}/V_{(t)}$, where "i" represent Xr_1, PHB, G, GLY, N_1, and (t) denotes a volume (V) at time "t".

$$m(\mathrm{CDM_1}) = m(\mathrm{Xr_1}) + m(\mathrm{PHB}) \tag{1}$$

$$\frac{\mathrm{d}m(\mathrm{Xr_1})}{\mathrm{d}t} = \begin{cases} 0, t \leqslant 5 \\ \mu_G \times m(\mathrm{Xr_1}) + \mu_{GLY} \times m(\mathrm{Xr_1}), t > 5 \end{cases} \tag{2}$$

$$\frac{dm(PHB)}{dt} = \mu_G \times m(Xr_1) \times Y_1 + q_G \times m(Xr_1) + q_{GLY} \times m(Xr_1) - \Sigma sampling \quad (3)$$

$$\frac{dm(G)}{dt} = -\mu_G \frac{m(Xr_1)}{Y_2} - \mu_G \frac{m(Xr_1) \times Y_1}{Y_3} - q_G \frac{m(Xr_1)}{Y_3} - b_1 \times m(Xr_1) - \Sigma sampling + \Sigma feed \quad (4)$$

$$\frac{dm(GLY)}{dt} = -q_{GLY} \frac{m(Xr_1)}{Y_4} - \mu_{GLY} \frac{m(Xr_1)}{Y_5} - \Sigma sampling + \Sigma feed \quad (5)$$

$$\frac{dm(N_1)}{dt} = -\mu_G \frac{m(Xr_1)}{Y_6} - \mu_{GLY} \frac{m(Xr_1)}{Y_7} + \mu_G \times m(Xr_1) \times C - \Sigma sampling + \Sigma feed \quad (6)$$

$$\mu_G = \mu_{G,max} \frac{G}{G + k_G} \times \frac{N_1}{N_1 + k_{N,G}} \quad (7)$$

$$\mu_{GLY} = \mu_{GLY,max} \frac{GLY}{GLY + k_{GLY}} \times \frac{N_1}{N_1 + k_{N,G}} \times \frac{k_i}{k_i + G} \quad (8)$$

$$q_G = q_{G,max} \frac{G}{G + k_G} \times \frac{k_{iN,G}}{k_{iN,G} + N_1} \quad (9)$$

$$q_{GLY} = q_{GLY,max} \frac{GLY}{GLY + k_{GLY}} \times \frac{k_{i,G}}{(G + k_{i,G})^r} \quad (10)$$

$$b_1 = b_{1,max} \frac{G}{G + k_G} \quad (11)$$

Changing of volume during fed-batch fermentation is defined with following differential equation (containing all feed inputs and sampling):

$$dV/dt = \Sigma F_G + \Sigma F_{GLY} + \Sigma F_{N1} - \Sigma sampling.$$

2.5.2. Mathematical model (FKM2) for PHBV production by C. necator on FAME/VA

System of mathematical model equations for fed-batch PHBV production from FAME combined with valeric acid (VA) includes six differential equations. Total biomass (CDM_2; Eq. (12)) consists of two different components: residual biomass (Xr_2) and PHBV. Residual biomass growth (Eq. (13)) includes time of lag phase of 37 h. Total PHBV copolymer mass is assumed to be the sum of HB mass and 3HV mass [$m(PHBV) = m(HB) + m(3HV)$]. Residual biomass mass balance equation (Eq. (13)) includes biomass growth and cell death processes. HB mass balance equation (Eq. (14)) includes growth associated and non-growth associated HB production on FAME. 3HV mass balance equation (Eq. (15)) includes non-growth associated 3HV production on VA. FAME mass balance equation (Eq. (16)) contains terms related to consumption for biomass growth, HB synthesis in nitrogen limited phase, maintenance energy production (b_2) and synthesis of HB during growth phase, respectively. The rate of mass change of *i*th biodiesel component ($C_{18:1}$, $C_{16:0}$, $C_{18:0}$, $C_{18:2}$, $C_{14:0}$, $C_{16:1}$, $C_{17:0}$, $C_{18:3}$, $C_{17:1}$, $C_{15:0}$, $C_{14:1}$, $C_{15:1}$, $C_{20:1}$, $C_{12:0}$, $C_{20:0}$) is set to be proportional to its mass fraction in the FAME mixture (Eq. (16a)). Valeric acid mass balance equation (Eq. (17)) includes consumption terms for: 3HV synthesis in nitrogen limited phase and maintenance energy for biomass. Nitrogen source mass balance equation (Eq. (18)) includes consumption term for biomass growth. Mass balance equations for all substrates contains terms related to reactor feeding and analytical sampling. In addition, equations for products (PHBV) contains terms related to analytical sampling procedures. Concentrations of substrates and products were calculated from mass to volume ratio according to following equation: $c_i = m_{i(t)}/V_{(t)}$; where "*i*" represent substrate or product, and (*t*) denotes a volume at time "*t*".

$$m(CDM_2) = m(Xr_2) + m(PHBV) \quad (12)$$

$$\frac{dm(Xr_2)}{dt} = \begin{cases} 0, t \leqslant 37 \\ \mu_{Fame} \times m(Xr_2) - k_d \times m(Xr_2) - \Sigma sampling, t > 37 \end{cases} \quad (13)$$

$$\frac{dm(HB)}{dt} = \mu_{FAME} \times m(Xr_2) \times Y_s + q_{FAME} \times m(Xr_2) - \Sigma sampling \quad (14)$$

$$\frac{dm(3HV)}{dt} = q_{VA} \times m(Xr_2) - \Sigma sampling \quad (15)$$

$$\frac{dm(FAME)}{dt} = -\mu_{FAME} \frac{m(Xr_2)}{Y_9} - q_{FAME} \frac{m(Xr_2)}{Y_{10}} - b_2 * m(Xr_2) - \mu * m(Xr_2) \frac{Y_8}{Y_{10}} - \Sigma sampling + \Sigma feed \quad (16)$$

$$\frac{dm(FAME)_i}{dt} = C \times \frac{dm(FAME)}{dt} \quad (16a)$$

$$\frac{dm(VA)}{dt} = -q_{VA} \frac{m(Xr_2)}{Y_{11}} - z_{VA} \times m(Xr_2) - \Sigma sampling + \Sigma feed \quad (17)$$

$$\frac{dm(N_2)}{dt} = -\mu_{VA} \frac{m(Xr_2)}{Y_{12}} - \Sigma sampling + \Sigma feed \quad (18)$$

Furthermore, mathematical model consist of 5 additional kinetic equations related to specific growth rate (μ_{FAME}), specific non-growth associated HB production rate on FAME (q_{FAME}), specific non-growth associated 3HV production rate on VA (q_{VA}), specific consumption rate of FAME for maintenance energy (b_2) and specific rate of VA consumption for maintennce energy (z_{VA}) (defined in Eqs. (19)–(23)).

$$\mu_{FAME} = \mu_{FAME,max} \frac{FAME}{FAME + k_{FAME}} \times \frac{N_2}{N_2 + k_{N,2}} \quad (19)$$

$$q_{FAME} = q_{FAME,max} \frac{FAME}{FAME + k_{FAME}} \times \frac{k_{iN,FAME}}{k_{iN,FAME} + N_{FAME}} \quad (20)$$

$$q_{VA} = q_{VA,max} \frac{VA}{VA + k_{VA}} \quad (21)$$

$$b_2 = b_{2,max} \frac{VA}{VA + k_{VA}} \quad (22)$$

$$z_{VA} = z_{VA,max} \frac{VA}{VA + k_{VA}} \quad (23)$$

Changing of volume during fed-batch fermentation is defined with following differential equation: $dV/dt = \Sigma F_{FAME} + \Sigma F_{VA} + \Sigma F_{N2} - \Sigma$ sampling (24).

2.5.3. Value of model parameters

Values of model parameters for FKM1 and FKM2 models are presented in Table 1.

2.5.4. Software package and integration methods

Established systems of mathematical differential equations related to models FMK1 and FMK2 were solved by Berkeley-

Table 1
Values of model parameters for both mathematical models (FKM1 and FKM2) obtained from experimental data by kinetic analysis and by parameter optimization procedures.

Symbol	Model	Value	Unit	Symbol	Model	Value	Unit
INIT V_1	FKM1	3.97	L	INIT V_2	FKM2	4.99	L
INIT $m(Xr_1)$	FKM1	13.58	g	INIT $m(Xr_2)$	FKM2	22.02	g
INIT m(G)	FKM1	164.86	g	INIT m(FAME)	FKM2	11.03	g
INIT m(GLY)	FKM1	1×10^{-5}	g	INIT m(VA)	FKM2	0	g
INIT $m(N_1)$	FKM1	3.88	g	INIT $m(N_2)$	FKM2	5.53	g
INIT m(PHB)	FKM1	1.18	g	INIT m(HB)	FKM2	5.48	g
$\mu_{G,max}$	FKM1	0.171	h^{-1}	INIT m(3HV)	FKM2	0	g
$\mu_{GLY,max}$	FKM1	0.01	h^{-1}	$\mu_{FAME,max}$	FKM2	0,046	h^{-1}
$q_{G,max}$	FKM1	0.162	h^{-1}	$q_{FAME,max}$	FKM2	0,07	h^{-1}
$q_{GLY,max}$	FKM1	0.038	h^{-1}	$q_{VA,max}$	FKM2	0.016	h^{-1}
$b_{GG,max}$	FKM1	0.19	h^{-1}	$b_{FAME,max}$	FKM2	0.013	h^{-1}
k_G	FKM1	0.1	$g\,L^{-1}$	k_{FAME}	FKM2	0.1	$g\,L^{-1}$
$k_{N,G}$	FKM1	0.24	$g\,L^{-1}$	$k_{N,FAME}$	FKM2	0.001	$g\,L^{-1}$
k_{GLY}	FKM1	11	$g\,L^{-1}$	k_{VA}	FKM2	1.256	$g\,L^{-1}$
$k_{i,G}$	FKM1	4.28×10^{-4}	$g\,L^{-1}$	$k_{iN,FAME}$	FKM2	0.0014	$g\,L^{-1}$
$k_{iN,G}$	FKM1	0.08	$g\,L^{-1}$	k_d	FKM2	0.01	$g\,L^{-1}$
r	FKM1	0.65	–	z_m	FKM2	0.1	h^{-1}
Y_1	FKM1	0.485	$g\,g^{-1}$	Y_8	FKM2	0.068	$g\,g^{-1}$
Y_2	FKM1	0.73	$g\,g^{-1}$	Y_9	FKM2	0.99	$g\,g^{-1}$
Y_3	FKM1	0.43	$g\,g^{-1}$	Y_{10}	FKM2	0.99	$g\,g^{-1}$
Y_4	FKM1	0.1	$g\,g^{-1}$	Y_{11}	FKM2	0.96	$g\,g^{-1}$
Y_5	FKM1	0.0841	$g\,g^{-1}$	Y_{12}	FKM2	7.26	$g\,g^{-1}$
Y_6	FKM1	9.8	$g\,g^{-1}$				
Y_7	FKM1	23.18	$g\,g^{-1}$				
C	FKM1	0.00965					

Table 2
Substrate feeding conditions of FAME, nitrogen and VA for *in silico* performed experiments by FKM2.

Experiment	Inflow					
	FAME		N		VA	
	10–12 ($g\,L^{-1}$)	1–2 ($g\,L^{-1}$)	Cont. feed	Limited feed	Puls feed	Cont. feed
MO1	+	–	+	–	+	–
MO2	–	+	+	–	+	–
MO3	+	–	–	+	+	–
MO4	–	+	–	+	+	–
MO5	+	–	+	–	–	+
MO6	–	+	+	–	–	+
MO7	+	–	–	+	–	+
MO8	–	+	–	+	–	+

Madonna quick solver (version 8.3.14) using fourth order Runge–Kutta numerical integration method for solving differential equations. Except kinetic parameters which where estimated from experimental data, model parameters were determined by Monte Carlo optimization method in order to reach the appropriate accordance between simulated curves and experimental data (minimization of objective function).

2.5.5. Process optimization procedures

GLY/G fermentation (FKM1) was *in silico* tested (optimized) as fed-batch type cultivation. During *in silico* optimization the nitrogen source (N_1) inflow was set to be proportional to the biomass growth rate. Glycerol concentration (GLY_0) in the feed stream was set to 200 $g\,L^{-1}$. In addition, a very low feed inflow was chosen ($F = 0.1\ L\,h^{-1}$, for applied batch volume $V_0 = 4$ L) and glucose concentrations in inflow were varied stepwise in the range ($G_0 = 10$–$100\ g\,L^{-1}$; step 1 and 20).

FAME/VA fermentation was *in silico* tested by simulation of eight different fed-batch cultivation procedures (MO1–MO8) using FKM2 model. In four of them *in silico* performed fermentations (MO1, MO3, MO5, MO7), concentration of FAME was hold in feeding phase in the range 10–12 $g\,L^{-1}$. In additional four (MO2, MO4, MO6 and MO8) FAME concentration in bioreactor was hold in lower range (1–2 $g\,L^{-1}$). This two feeding strategies were combined with two additional conditions regarding nitrogen and valeric acid concentration in the feed stream. Nitrogen source (N_2) was set as continuous inflow during the whole time of MO1, MO2, MO5 and MO6 *in silico* fermentations. In contrary, in the MO3, MO4, MO7, MO8 *in silico* experiments, nitrogen inflow was stopped when its concentration dropped below 0.01 $g\,l^{-1}$ (system become nitrogen limited; Table 2). In addition, valeric acid feeding was performed in two different ways: threefold stepwise addition (in MO1, MO2, MO3, MO4) and continuous addition during FAME feeding phase in MO5, MO6, MO7, MO8 (Table 2). Also, all eight *in silico* fermentations were performed without relatively long lag phase (approximately 37 h) that was experimentally observed, because this problem must be solved by appropriate inoculum preparation.

3. Results and discussion

3.1. Results of C. necator cultivation on GLY/G and mathematical modeling by FKM1 model

Glycerol as the waste material from biodiesel production is usually burned in the biodiesel factories in order to produce the necessary heat for support of esterification process. Otherwise, this organic compound can be used for biotechnological production of bulk chemicals (i.e. 1,3-propanediol, PHB) or can be refined and

used as chemical solvent. In this work the biotechnological conversion of glycerol in PHB by *C. necator* was investigated. As it was reported in the past (Kaddor and Steinbüchel, 2011), mentioned strain is growing slower on glycerol then on glucose. Therefore, GLY/G fermentation was performed with presence of glucose in the broth in the first (growth) phase of fermentation. Glycerol was added later, at the moment when nitrogen source was almost depleted. This way, an intention was to achieve rapid growth of biomass on glucose and after that to have PHB production from glycerol. Additionally, the low structured mathematical formal kinetic model (FKM1) was established in order to simulate different cultivation situations and to improve PHB production (Fig. 2a and b). Based on experimental and simulated results, some conclusions can be formulated for performed PHB production on GLY/G by *C. necator*:

(i) As expected, under nitrogen limited conditions metabolism of *C. necator* redirects a part of metabolic carbon flux (essentially needed for the biomass growth!) towards PHB synthesis. This well-known mechanism was built in the FKM1 model and has justified its existence. The presence of N_1 source was drastically reduced in the time period of 18–25th hour of fermentation (Fig. 2b). In the same time, that was the period of intensive glucose consumption and feeding. After N_1 depletion, an increased synthesis of PHB on glucose was observed.

(ii) It seems that applied glucose concentration in some degree inhibit glycerol consumption for PHB production. The evidence for just mentioned statement is the presence of "saw tooth" shaped curves of glycerol and glucose concentrations (Fig. 2b). Careful observation of these curves shows that glycerol consumption was always practically stopped when the glucose concentration has reached desired level (local peak!) caused by feeding. After glucose was depleted, the consumption of glycerol was enhanced. The explanation for this includes the fact that the first enzymatic step of glycerol consumption in bacteria is the glycerol kinase reaction (synthesis of glycerol-3-phosphate that is further converted to the dihydroxyacetone phosphate /DHAP/ a substrate of glycolysis). Its high intracellular pool acts as the negative feed-back controller of glycerol consumption (Schryvers et al., 1978). Without installing of inhibited glycerol consumption (by glucose) in the model equations, it was impossible to achieve the accordance between the experiment and stimulation.

(iii) The observed PHB production rate was higher on glucose then on glycerol. In the non-growth period of PHB synthesis the slopes of parts of PHB concentration curve were steeper when glucose was present in the broth if compared with the time range when only glycerol was consumed.

(iv) Experimental and simulated glucose concentrations (Fig. 2a) indicate that addition of glucose should be optimized. It seems that before glycerol addition and especially after depletion of nitrogen source, glucose was totally consumed in desired time periods. That means that the growth was briefly interrupted and the biomass was a part of time under limitation of C-source.

Guided by above conclusions it was assumed that it is necessary to enhance the glycerol consumption rate for PHB synthesis. To achieve this target and to reduce necessary experimental setup, the *in silico* fermentations were performed using FKM1 model. In those optimizations continuous inflow of both carbon sources (G and GLY) in one feed stream (with different mass ratio) were applied. The main goal was to find the optimal G/GLY/N_1 ratio for growth phase and for PHB synthesis phase. The target of *in silico* optimization of GLY/G fermentation was to reach a glucose concentration in the bioreactor in the range from 0.01 to 0.1 g L^{-1}, applicable for the PHB synthesis phase. It was assumed that such glucose concentration has to be high enough to support some degree of precursors and energy production in cells. At the same time, this concentration should not be high to block the glycerol consumption (i.e. it should be without or with weak inhibitory influence on the PHB synthesis from glycerol). Results of these *in silico* experiments (process optimization) are presented in Table 3 as well as in Fig. 2c and d.

Fig. 2a contains very useful results, important for the elucidation of experimental results presented above (Fig. 2c). Simulated glycerol concentration curves for all *in silico* experiments are very near and show a continuous increasing in the feeding phase up to 100 g L^{-1}. This concentration range is inhibitory for producing microorganism. The *in silico* glucose concentrations in feed phase are very low (despite continuous feed!) and in accordance (or lower!) than the planned range for glucose concentration of 0.01 to 0.1 g L^{-1} (Table 3). *In silico* produced Xr_1 has reached values close (or equal) to experimental data if glucose concentration in the feed stream was hold in the range 55–100 g L^{-1}. The price for this was *in silico* enhanced N_1 source concentration and therefore the lower mass of PHB than in real experiment. Furthermore, yield coefficients of PHB toward glycerol ($Y_{4,stat,phase}$) are in all *in silico* experiments (except those with 10 g L^{-1} glucose in the feed stream) significantly higher (Table 3) than theoretical (0.56 g g^{-1}). The reason is the dominant share of PHB originated from glucose in the whole PHB mass which was taken in the account. Based on results of *in silico* experiments it can be concluded that despite low glucose concentrations in the broth (Table 3) the glycerol conversion toward PHB was not enhanced (under kinetical properties of used *C. necator* !). These results as well as the behavior of this strain in experiment (i.e. glycerol consumption negatively influenced by present glucose) indicate that the problem lie in very high sensitivity of glycerol kinase and glycerol-3-phosphate dehydrogenase on intracellular metabolites originated from glucose. Mentioned influence is so strong that lowering of glucose concentration practically does not have a positive influence on the glycerol consumption rate, so the process cannot be improved on this way. The problem could be perhaps solved by improvement of capacity of transport system for glycerol.

3.2. Results of C. necator cultivation on FAME/VA and mathematical modeling by FKM2 model

FAME from animal waste is a multisubstrate C-source composed of different fatty acids methyl esters (saturated and unsaturated) with different number of carbon atoms in chain. In FAME (biodiesel) that was used for this fermentation the most represented fatty acids esters are oleic ($C_{18:1}$; 39.61%), palmic ($C_{16:0}$; 27.47%) and stearic fatty acid methyl ester ($C_{18:0}$; 18.39%), that is summarized 85.47% of whole FAMEs. The rest of (14.53%) include esters of fatty acids $C_{18:2}$ (4.6%), $C_{14:0}$ (2.87%), $C_{16:1}$ (2.73%), $C_{17:0}$ (1.27%) and among them 3.06% of total are underrepresented esters of fatty acids $C_{18:3}$ (0.92%), $C_{17:1}$ (0.64%), $C_{15:0}$ (0.56%), $C_{14:1}$ (0.36%), $C_{15:1}$ (0.22%), $C_{20:1}$ (0.17%), $C_{12:0}$ (<0.1%) and $C_{20:0}$ (<0.1%). Such complex substrate is from metabolic and kinetic point of view very unpredictable and can result with different percentage of PHBV in the cells. Results of simulation of fed-batch cultivation by *C.necator* on FAME combined with valeric acid (VA) achieved by FKM2 model are presented on Fig. 3. Results of application of established mathematical model (FKM2) on FAME/VA fed- batch fermentation indicates that this model fit very well experimental data for residual biomass (Xr_2) and for PHBV. A little less but still useful agreement is achieved for total biodiesel concentration curve in growth phase. In the second part of cultivation

Table 3
Quantitative indicators of basic G/GLY experiment and *in silico* fermentations.

	Unit	EXP	FKM1	Optimization of GLY/G fermentation				
				Go = 10 g L^{-1}	Go = 32 g L^{-1}	Go = 55 g L^{-1}	Go = 77 g L^{-1}	Go = 100 g L^{-1}
INIT m(G)	g	165	165	165	165	165	165	165
$m(G)_{ADDED}$	g	660	660	42.3	137.5	232.66	327.8	423
$m(G)_{USED}$	g	825	825	207.3	302.5	397.5	492.8	588
$m(GLY)_{ADDED}$	g	195	195	846	846	846	846	846
$m(GLY)_{USED}$	g	88	88	35	15.5	10.5	8	6.5
INIT m(PHB)	g	1.18	1.18	1.18	1.18	1.18	1.18	1.18
$m(PHB)_{t = 15h}$	g	23.25	18.6	18.95	18.95	18.95	18.95	18.95
$m(PHB)_{final}$	g	164.39	168	27.42	42.5	62.69	87.46	113.64
INIT m(Xr)	g	13.58	13.58	13.58	13.58	13.58	13.58	13.58
$m(Xr)_{t = 15h}$	g	54.68	51.63	52.52	52.42	52.42	52.42	52.42
$m(Xr)_{final}$	g	90.31	97.3	64.58	80.41	88.96	92.1	93.89
$m(CDM)_{final}$	g	254.7	265.3	92	122.91	151.65	179.56	207.53
$Y_{P/G\ exp.phase}$	g g^{-1}	0.134	0.105	0.108	0.108	0.108	0.108	0.108
$Y_{Xr/G\ exp.phase}$	g g^{-1}	0.248	0.231	0.235	0.235	0.235	0.235	0.235
$Y_{P/GLY\ stat.phase}$	g g^{-1}	1.604	1.698	0.242	1.519	4.166	8.564	14.609
% PHB_{final}	–	64.54	63.3	29.77	34.56	41.35	48.72	54.76
$G_{stat.phase}$	g L^{-1}		Variable 23.04–0	0.0031–0.0035	0.009–0.012	0.014–0.022	0.018–0.034	0.023–0.042

(phase of N_2 limited, intensive PHBV synthesis without biomass growth), a better agreement of the FAME time course curve with experimental data was obtained. Two important facts can be highlighted: (I) the model provides good results for the experimentally determined specific growth rate (μ_{FAME} = 0.036 h^{-1}) which is actually the difference between maximal specific growth rate ($\mu_{FAME,max}$ = 0.046 h^{-1}) and specific death rate (k_d = 0.01 h^{-1}); (II) the applied lag-phase of 37 h fits well with the subsequent growth kinetic as well as with the time courses of PHBV synthesis.

Special attention has to be devoted to the behavior of the simulated N_2 curve (Fig. 3). This curve is in some disagreement with

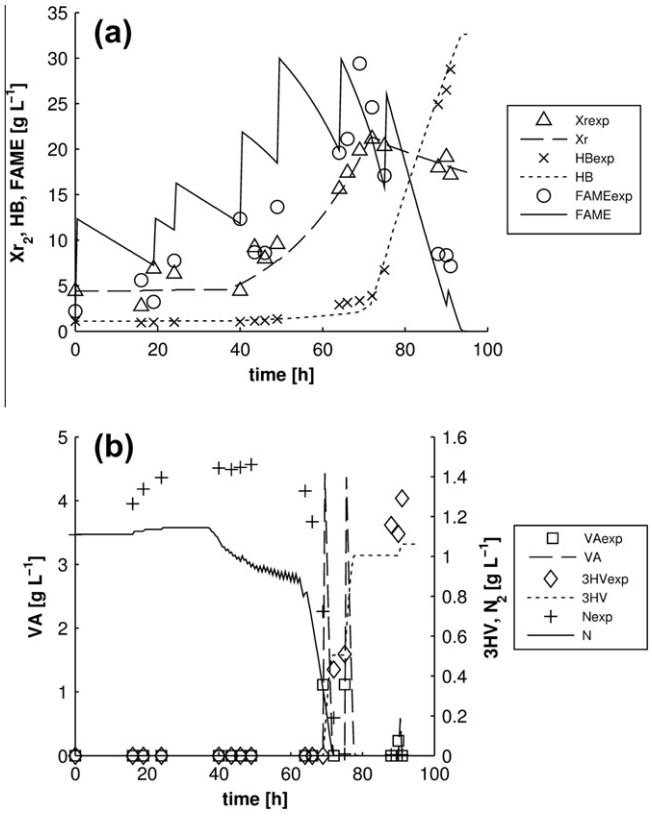

Fig. 3. (a and b) Experimental and simulated data (FKM2) of PHBV (HB + 3HV) production on FAME/VA by *Cupriavidus necator* DSM 545: model validation.

experimental data, but fits excellent the time point of transition from growth-associated to growth non-associated PHBV synthesis. An interesting result of simulation was achieved for depletion of valeric acid (VA). If the rate of its depletion for 3HV synthesis was stoichiometrically calculated and applied in the model, the agreement of experimental 3HV data with model simulation was miserable. In contrary, when the consumption of this carbon substrate for the maintenance energy (b_2) was introduced in the model, both curves (for VA and 3HV) were in good agreement with experimental data. This situation indicates that VA is easier degradable then FAME from biodiesel and therefore metabolized for energy production also. Looking at performed fermentation, it can be impeaching that FAME concentration was frequently switched from high to low values (because of stepwise intermittent addition). This can be an inhibitory factor for PHBV synthesis and for biomass growth (concentration is many times changed from substrate inhibition to starvation level).

Results of simulation related to degradation of different FAME during *C. necator* cultivation (Fig. 4) indicate that there is no big difference in the consumption rate of mcl-FAMEs present in the biodiesel. An assumption that consumption rates of diverse FAMEs are proportional to its mass fraction in the mixture has been shown as correct when was applied in the FKM2 model. Despite relatively complex substrate, FKM2 fits well experimental concentrations of a number of FAME components, especially those with low content in the mixture (Fig. 4). These results are the strong indication that diverse FAME compete for transport through the cell membrane as well as for the place in metabolic reactions. Relatively long lag phase (37 h) and rising of FAME concentrations in the fermentation during feeding phase are strong indicators that this microbial culture must be adapted on applied biodiesel concentrations. An avoiding of substrate inhibition can be performed in the fed-batch process similar as in the chemostat: FAME concentration must be held on desired level by addition of substrate in such quantities that are consumed during desired time period. This idea was *in silico* tested by application of intermittent inflow of substrates (Table 2) on the two different ways: the FAME concentration was kept in two different ranges (10–12 and 1–2 g L^{-1}). The typical behaviors of such system are presented on Fig. 5a and Fig. 5b. (MO1 experiment) and results of simulation are in Table 4. Results presented in Table 4 show the whole complexity of such interaction of biodiesel substrate mixture and metabolic system. Bold and underlined numbers are maximums achieved by simulation when different fermentation conditions (FAME concentration, N_2

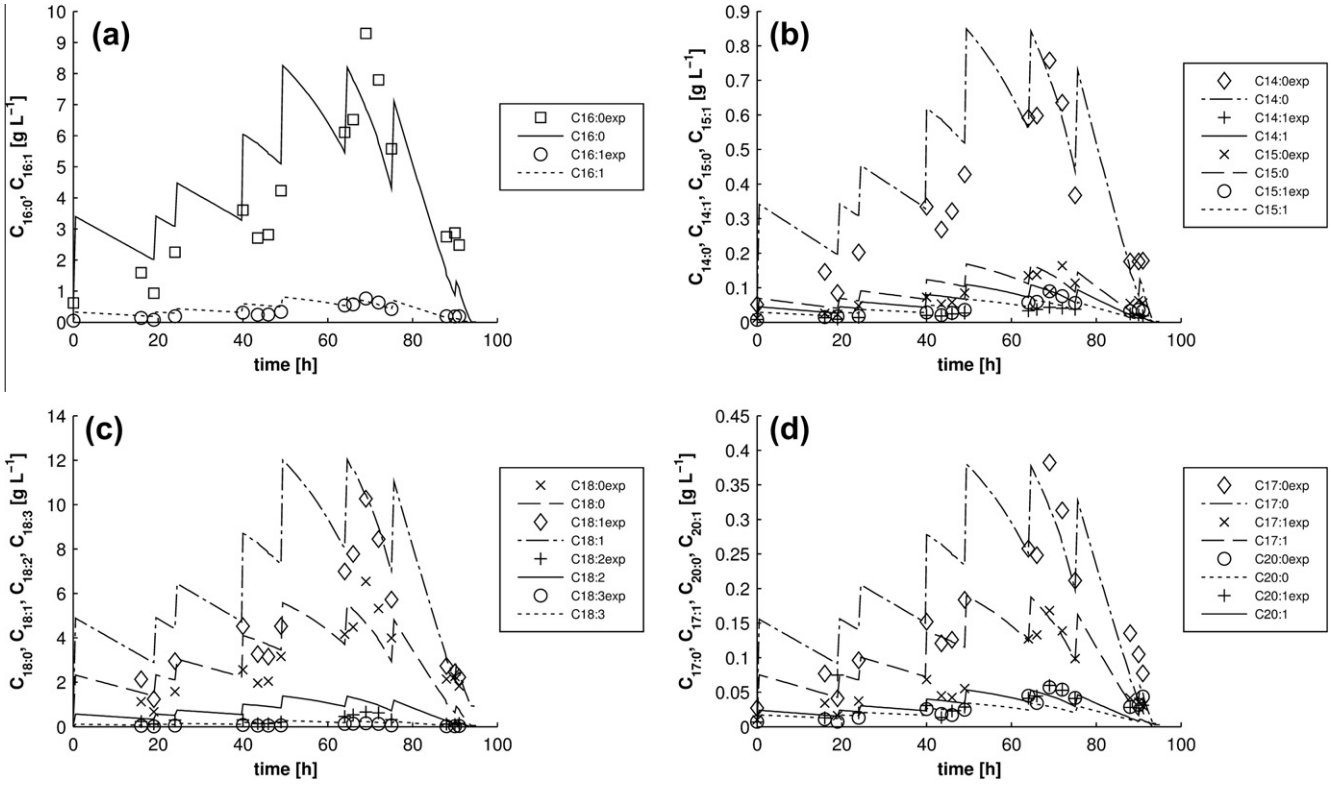

Fig. 4. Simulated and experimental data for degradation of different FAME components (from bio-diesel) during *Cupriavidus necator* DSM 545 cultivation.

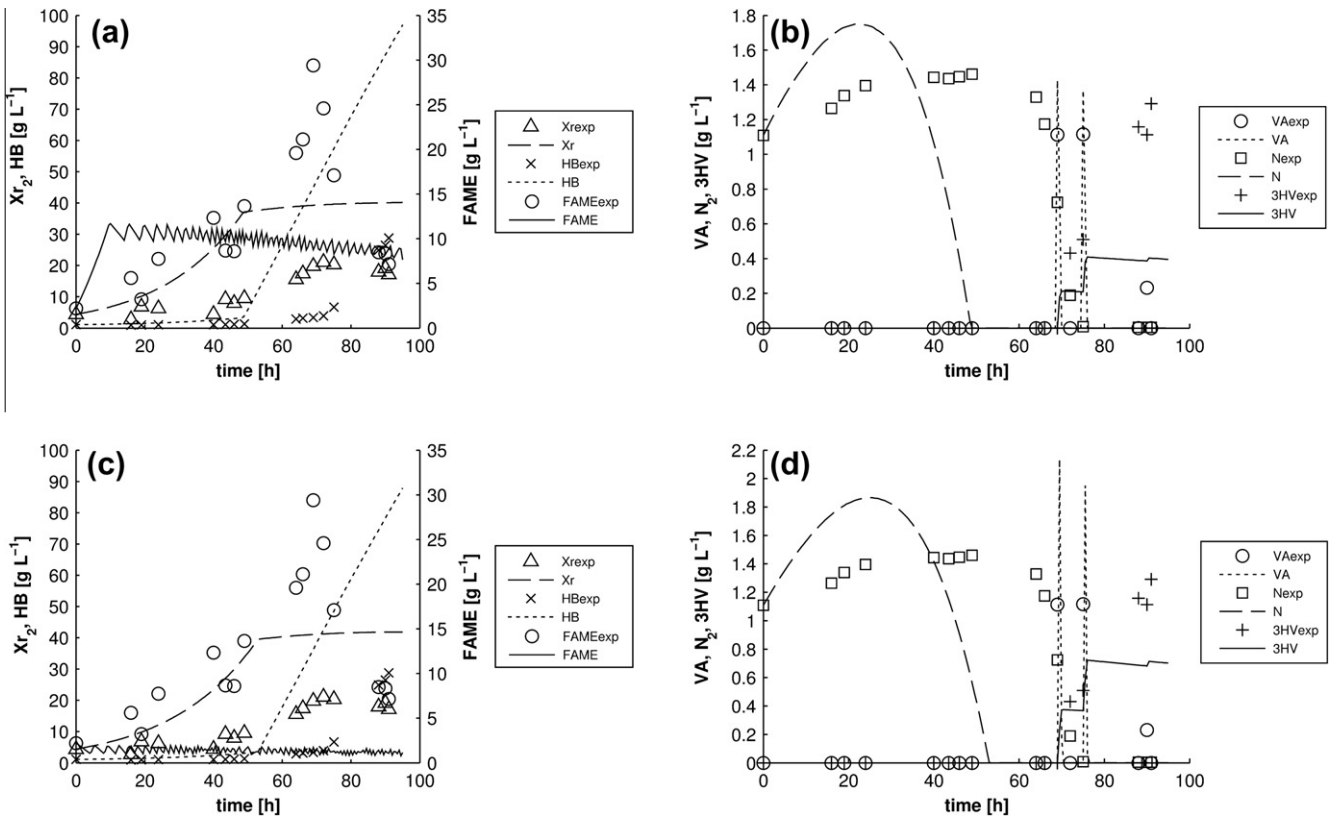

Fig. 5. Presentation of different *in silico* fermentations: (a and b) MO1 and (c and d) MO2. Experimental data from basic fermentation (FAME/VA) are added for comparison.

feeding, VA feeding) were *in silico* applied. Diverse variables reach maximum values at completely different conditions (dependent on relations between FAME, N_2 and VA). Changed feed streams for FAME and N_2 source (Table 2), have *in silico* yielded better results than in basic experiment (Fig 3): higher concentrations of Xr_2 and PHBV were achieved with minimized specific death rate (k_d).

Table 4
Results of FAME/VA fermentation for basic experimental and *in silico* performed fermentations.

	Exp. data	Optimized results								Unit
		MO1	MO2	MO3	MO4	MO5	MO6	MO7	MO8	
CDM_{final}	47.23	126.00	118.8	106.44	100.1	90.54	85.83	82.24	77.75	g L^{-1}
Xr_{final}	17.18	38.17	40.03	22.22	23.41	24.39	25.98	15.36	16.35	g L^{-1}
$PHBV_{final}$	30.05	87.83	78.77	84.22	76.69	66.15	59.85	66.88	61.4	g L^{-1}
HB_{final}	28.76	87.14	78.05	83.48	75.93	60.59	54.35	61.97	56.54	g L^{-1}
$3HV_{final}$	1.29	0.69	0.72	0.74	0.76	5.56	5.5	4.91	4.86	g L^{-1}
m(Xr)	72.84	245.82	251.45	136.13	140.13	245.87	251.83	136.13	140.13	g
m(PHBV)	127.4	565.71	494.8	515.88	459.06	666.7	580.18	592.66	526.08	g
m(HB)	121.94	561.24	490.3	511.38	454.53	610.63	526.85	549.15	484.47	g
m(3HV)	5.46	4.47	4.5	4.50	4.53	56.06	53.33	43.51	41.61	g
V_{final}	4.26	6.44	6.28	6.13	5.99	10.08	9.69	8.86	8.57	L
%PHBV	63.62	69.71	66.31	79.12	76.61	73.06	69.73	81.32	78.97	%
%3HV/PHBV	4.29	1	0.9	0.87	0.99	8.4	9.19	7.34	7.9	%
Pr_{total}	0.330	0.965	0.866	0.925	0.843	0.727	0.690	0.735	0.674	g L^{-1} h^{-1}

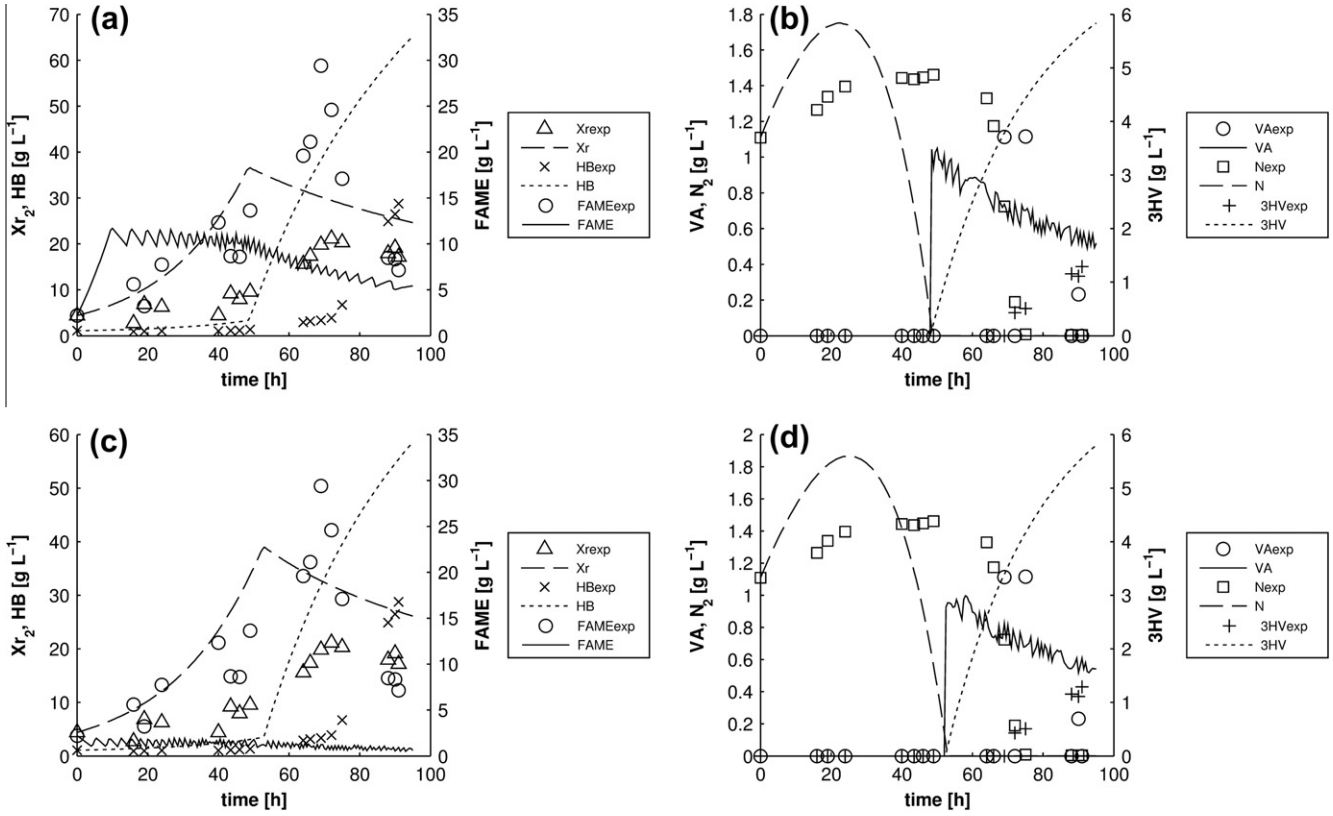

Fig. 6. Presentation of different *in silico* fermentations: (a and b) MO5 and (c and d) MO6. Experimental data from basic fermentation (FAME/VA) are added for comparison.

Further step in improving of this cultivation was testing of Xr_2 and PHBV synthesis rates under exposition of biomass to lower FAME concentrations, so MO2 *in silico* experiment was performed (Fig. 5c and d) with intermittent inflow of FAME in the range between 1 and 2 g L^{-1} (Table 2). Comparing results of MO2 (Fig. 5c) with results of MO1 fermentation (Fig. 5a and b) it can be observed that *in silico* performed fermentation (MO2) has resulted with 10 g L^{-1} less HB and with 2 g L^{-1}more Xr_2. Furthermore, the redirection of carbon flux toward PHBV caused by limitation of N_2 source occur 4 h later (Table 4). Next *in silico* cultivation (MO3, graphic not showed) was simulated under conditions of maximized concentration of FAME in bioreactor at 12 g L^{-1}. Also, N source inflow has been stopped (unlike in MO1) when concentration of N dropped on almost zero (after approximately 49 h systems has become N limited). This *in silico* experiment (MO3) resulted with 5 g L^{-1} lower PHBV concentration then in MO1 (Table 4). In MO3 *in silico* experiment, residual biomass (Xr_2) reaches 38 g L^{-1} but in the N limited part of cultivation the rate of cell death was significant. *In silico* experiment (MO4) that was performed with lower FAME concentration (Table 2) and with limitation of N inflow in the PHBV production phase, the produced PHA concentration was even lower (graphic not showed, Table 4) then in MO3 fermentation. In real experiment (Fig. 3) as well as in *in silico* experiments MO1, MO2, MO3 and MO4 valeric acid was consumed too fast and in the same time there was not enough synthesized 3HV. So, it was meaningful to optimize the inflow of VA and intermittent inflow of VA. This type of VA inflow (concentration was kept in the range 0.45–1.1 g L^{-1} of non-toxic concentrations of VA on *C. necator*) was *in silico* combined with two levels of FAME concentration [between 10–12 g L^{-1} (MO5, MO7) and 1–2 g L^{-1} (MO6, MO8)],

and additionally with two different N source inflows (full time continuous and interrupted in PHA synthesis phase).

Results of MO5 and MO6 *in silico* experiments with intermittent inflow of FAME combined with continuous inflow of N and with intermittent inflow of VA are presented on Fig. 6. It can be seen that simulated intermittent inflow of VA influence positively on poly-3HV synthesis. In MO5 final concentration of 3HV (5.56 g L^{-1}) was higher then in MO1-MO4 and higher than in real experiment (1.29 g L^{-1}). The MO6 *in silico* experiment (FAME 1–2 g L^{-1}; continuous N inflow; VA intermittent inflow) was ended with the final concentration of 3HV of 5.5 g L^{-1} and with the highest 3HV content 9.2% in total PHBV. *In silico* performed experiments MO7 (FAME 10–12 g L^{-1}) and MO8 (FAME 1–2 g L^{-1}) combined with intermittent VA inflow and with N limitation (N inflow was stopped in the PHBV production phase) did not ended with better results concerning 3HV content in PHA (graphic is not showed). Furthermore, the *in silico* fermentations MO5 and MO6 have been resulted with higher 3HV concentration and 3HV content then in real basic experiment (Fig. 3) as well as *in silico* simulation MO1 (Fig. 5 a and b).

Based on results obtained from *in silico* fermentation (MO1–MO8) it seems that higher concentration of FAME (10–12 g L^{-1}) in the inlet stream will have a positive influence on the total yield of PHBV and will result in better productivity with a higher mass fraction of PHBV. Biomass degradation in the PHBV synthesis phase can be prevented if continuous inflow of nitrogen source is chosen with carefully selected concentration in the inlet stream. This will lead to better residual biomass (Xr_2) production with minor influence on PHBV synthesis rate. This will also decrease PHBV/CDM_2 ratio and increase the total mass of produced PHBV. At the end, based on FKM2, there is a evidence that a part of valeric acid (VA) will be metabolized for energy production faster than FAME from biodiesel. Also, production of 3HV will be possible in *C. necator* DSM 545 only if VA is used as carbon source (3HV component was not detected when in broth only FAME without VA was present). Controlled inflow of VA and holding this substrate at a desirable level will have positive influence on the 3HV content in PHBV.

4. Conclusions

Both mathematical models match well experimental results. When *C. necator* is cultivated on G/GLY, the glycerol consumption is practically full blocked by low glucose concentration ($k_{i,G}$ = 4.28 - $\times 10^{-4}$ g L^{-1}), so the improvement of PHB synthesis from glycerol by lowering of G/GLY ratio is impossible. Long lag-phase obtained when cultivation was performed on FAME indicated the necessary adaptation of culture on FAME. Consumption rates of different FAMEs (C_{14}–C_{20}) are proportional to its mass fraction (competitiveness!). Applied concentration of FAME (10–12 g L^{-1}) positively influenced on PHBV synthesis. Higher HV/PHBV ratio can be achieved by increasing of VA concentration.

Acknowledgements

This work was supported by the Collaborative European Union 7th Framework Project ANIMPOL (Biotechnological conversion of carbon containing wastes for eco-efficient production of high added value products; Grant agreement no.: 245084).

References

Aldor, I.S., Keaslingy, J.D., 2003. Process design for microbial plastic factories: metabolic engineering of polyhydroxyalkanoates. Curr. Opin. Biotechnol. 14, 475–483.

Braunegg, G., Sonnleitner, B., Lafferty, R.M., 1978. A rapid gas chromatographic method for the determination of poly-(β-hydroxy-butyric) acid in microbial biomass. Eur. J. Appl. Microbiol. Biotechnol. 6, 29–37.

Braunegg, G., Koller, M., Varila, P., Kutschera, C., Bona, R., Hermann, C., Horvat, P., Neto, J., Pereira, L., 2007. Production of plastics from waste derived from agrofood industry. In: Fornasiero, P., Graziani, M. (Eds.), Renew. Res. Renew. Energy. University of Trieste, Trieste, Italy, pp. 119–135.

Brigham, C.J., Budde, C.F., Holder, J.W., Zeng, Q., Mahan, A.E., Rha, C., Sinskey, A.J., 2010. Elucidation of β-oxidation pathways in *Ralstonia eutropha* H16 by examination of global gene expression. J. Bacteriol. 192 (20), 5454–5464.

Cavalheiro, J.M.B.T., de Almeida, M.C.M.D., Grandfils, C., da Fonseca, M.M.R., 2009. Poly(3-hydroxybutyrate) production by *Cupriavidus necator* using waste glycerol. Process Biochem. 44, 509–515.

Chakraborty, P., Gibbons, W., Muthukumarappan, K., 2009. Conversion of volatile fatty acids into polyhydroxyalkanoate by *Ralstonia eutropha*. J. Appl. Microbiol. 106, 1996–2005.

Du, G., Si, Y., Yu, J., 2001. Inhibition by medium-chain-length fatty acids of formation of polyhydroxyalkanoates from volatile fatty acids by Ralstonia eutropha. Biotechnol. Lett. 23, 1613–1617.

Gorenflo, V., Schmack, G., Vogel, R., Steinbuchel, A., 2001. Development of a process for the biotechnological large-scale production of 4-hydroxyvalerate-containing polyesters and characterization of their physical and mechanical properties. Biomacromolecules 2, 45–57.

Kaddor, C., Steinbüchel, A., 2011. Implications of Various Phosphoenolpyruvate-Carbohydrate Phosphotransferase System Mutations on Glycerol Utilization and Poly(3-hydroxybutyrate) Accumulation in *Ralstonia eutropha* H16 AMB Express 1:16.

Kelley, A.S., Mantzaris, N.V., Daoutidis, P., Srienc, F., 2001. Controlled synthesis of polyhydroxyalkanoic (PHA) nanostructures in *R. eutropha*. Nano Lett. 1 (9), 481–485.

Khanna, S., Srivastava, A.K., 2005. Recent advances in microbial polyhydroxyalkanoates. Process Biochem. 40, 607–619.

Koller, M., Bona, R., Braunegg, G., Hermann, C., Horvat, P., Kroutil, M., Martinz, J., Neto, J., Pereira, L., Varila, P., 2005. Production of polyhydroxyalkanoates from agricultural waste and surplus materials. Biomacromolecules 6 (2), 561–565.

Küng, W., 1982. Wachstum und Poly-D-(-)-hydroxybuttersäure-Akkumulation bei *Alcaligenes latus*. Diploma Thesis, Graz University of Technology, Austria.

Lageveen, R.G., Huisman, G.W., Preusting, H., Ketelaar, P., Eggink, G., Witholt, B., 1988. Formation of polyesters by *Pseudomonas oleovorans*: effect of substrates on formation and composition of poly-(R)-3-hydroxyalkanoates and poly-(R)-3-hydroxyalkenoates. Appl. Environ. Microbiol. 54, 2924–2932.

Lee, S.Y., 1996. Plastic bacteria?: Progress and prospects for polyhydroxyalkanoate production in bacteria. Trends Biotechnol. 14, 431–438.

Lefebvre, G., Rocher, M., Braunegg, G., 1997. Effects of low dissolved-oxygen concentrations on poly-(3-hydroxybutyrate-*co*-3-hydroxyvalerate) production by *Alcaligenes eutrophus*. Appl. Environ. Microbiol. 63 (3), 827.

Lemos, P.C., Serafim, L.S., Reis, M.A.M., 2006. Synthesis of polyhydroxyalkanoates from different short-chain fatty acids by mixed cultures submitted to aerobic dynamic feeding. J. Biotechnol. 122, 226–238.

Madison, L.L., Huisman, G.W., 1999. Metabolic engineering of poly(3-hydroxyalkanoates): from DNA to plastic. Microbiol. Mol. Biol. Rev. 63 (1), 21–53.

Moser, A., 1988. Bioprocess Technology: Kinetics and Reactors. Springer, Vienna.

Raberg, M., Peplinski, K., Heiss, S., Ehrenreich, A., Voigt, B., Döring, C., Bömeke, M., Hecker, M., Steinbüchel, A., 2011. Proteomic and transcriptomic elucidation of the mutant *Ralstonia eutropha* $G^{+}1$ with regard to glucose utilization. Appl. Environ. Microbiol. 77 (6), 2058–2070.

Reinecke, F., Steinbuchel, A., 2009. *Ralstonia eutropha* strain H16 as model organism for PHA metabolism and for biotechnological production of technically interesting biopolymers. J. Mol. Microbiol. Biotechnol. 16, 91–108.

Schryvers, A., Lohmeier, E., Weiner, J.H., 1978. Chemical and functional properties of the native and reconstituted forms of the membrane-bound, aerobic glycerol-3-phosphate dehydrogenase of *Escherichia coli*. J. Biol. Chem. 253, 783–788.

Steinbüchel, A., Valentin, H.E., 1995. Diversity of polyhydroxyalkanoic acids. FEMS Microbiol. Lett. 128, 219–228.

Steinbüchel, A., Doi, Y., 2001. Biopolymer, Volume 3b, Polyesters II, properties and chemical synthesis. Wiley-VCH, Weinheim, 2001.

Steinbüchel, A., Lütke-Eversloh, T., 2003. Metabolic engineering and pathway construction for biotechnological production of relevant polyhydroxyalkaonates in microorganism. Biochem. Eng. J. 16, 81–96.

Sudesh, K., Abe, H., Doi, Y., 2000. Synthesis, structure and properties of polyhydroxyalkanoates: biological polyesters. Prog. Polym. Sci. 25, 1503–1555.

Sweet, G., Gandor, C., Voegele, R., Wittekindt, N., Beuerle, J., Truniger, V., Lin, E.C.C., Boos, W., 1990. Glycerol facilitator of *Escherichia coli*: cloning of glpF and identification of the glpF product. J. Bacteriol. 172, 424–430.

Tanadchangsaeng, N., Yu, J., 2012. Microbial synthesis of polyhydroxybutyrate from glycerol: gluconeogenesis, molecular weight and material properties of biopolyester. Biotechnol. Bioeng. 109, 2808–2818.

Vandamme, P., Coenye, T., 2004. Taxonomy of the genus *Cupriavidus*: a tale of lost and found. Int. J. Syst. Evol. Microbiol. 54, 2285–2289.

Yu, J., Si, Y., 2004. Metabolic carbon fluxes and biosynthesis of polyhydroxyalkanoates by *Ralstonia eutropha* on short chain fatty acids. Biotechnol. Prog. 20, 1015–1024.

Wu, S.C., Liou, S.Z., Lee, C.M., 2012. Correlation between bio-hydrogen production and polyhydroxybutyrate (PHB) synthesis by *Rhodopseudomonas palustris* WP3-5. Bioresour. Technol. 113, 44–50.

You, S.-J., Tsai, Y.-P., Cho, B.-C., Chou, Y.-H., 2011. Metabolic influence of lead on polyhydroxyalkanoates (PHA) production and phosphate uptake in activated sludge fed with glucose or acetic acid as carbon source. Bioresour. Technol. 102, 8165–8170.

Zinn, M., Witholt, B., Egli, T., 2004. Dual nutrient limited growth: models, experimental observations, and applications. J. Biotechnol. 113, 263–279.

Further reading

Tyburczy, C., Delmonte, P., Fardin-Kia, A.R., Mossoba, M.M., Kramer, J.K., Rader, J.I., 2012. Profile of trans Fatty Acids (FAs) Including Trans Polyunsaturated FAs in Representative Fast Food Samples. Journal of Agricultural and Food Chemistry 60 (18), 4567–4577.